Optical Quality and Depth-of-field of Eyes Implanted With Spherical and Aspheric Intraocular Lenses

Susana Marcos, PhD; Sergio Barbero, PhD; Ignacio Jimenez-Alfaro, MD, PhD

ABSTRACT

PURPOSE: To compare experimental optical performance in eyes implanted with spherical and aspheric intraocular lenses (IOLs).

METHODS: Corneal, total, and internal aberrations were measured in 19 eyes implanted with spherical (n=9) and aspheric (n=10) IOLs. Corneal aberrations were estimated by virtual ray tracing on corneal elevation maps, and total aberrations were measured using a second-generation laser ray tracing system. Corneal and total wave aberrations were fit to a Zernike polynomial expansion. Internal aberrations were measured by subtracting corneal from total wave aberrations. Optical performance was evaluated in terms of root-mean-square (RMS) wavefront error and Strehl ratio (estimated from the modulation transfer function). Depth-of-field was obtained from through-focus Strehl estimates from each individual eye.

RESULTS: Corneal aberrations increased after IOL implantation, particularly astigmatism and trefoil terms. Third and higher order RMS (and the corresponding Strehl ratio) were significantly better in eyes with aspheric IOLs than with spherical IOLs; however, this tendency was reversed when astigmatism was included. Spherical aberration was not significantly different in eyes with aspheric IOLs, whereas it was significantly positive in eyes with spherical IOLs. Third order aberrations were not significantly different across groups. Depth-of-field was significantly larger in eyes with spherical IOLs. Spherical IOLs showed better absolute optical quality in the presence of negative defocus >1.00 D.

CONCLUSIONS: Our study shows a good degree of compensation of the corneal spherical aberration in eyes implanted with aspheric IOLs, as opposed to eyes implanted with spherical IOLs. Other sources of optical degradation, both with aspheric and spherical IOLs, are non-symmetric preoperative corneal aberrations, incision-induced aberrations, and third order internal aberrations. Although best corrected optical quality is significantly better with aspheric IOLs, tolerance to defocus tended to be lower. [*J Refract Surg*. 2005;21:xxx-xxx.]

The recent application of wavefront sensing technology has provided a deeper insight into the optical outcomes of surgical techniques, such as corneal refractive surgery[1,2] and cataract surgery.[3] The sources of optical degradation inherent to the techniques have been identified[4] and correlated to the patient's vision,[5] resulting in potential improvements of the techniques. Today, many different intraocular lenses (IOLs) are available for implantation in cataract surgery, and continuous efforts are made to reduce the incision size through which the IOL is implanted.

The measurement of optical aberrations in the normal eye is also expanding the knowledge of the optical properties of the ocular components of the accommodated and unaccommodated eye,[6] emmetropic or ametropic eye,[7-9] the young and aging eye,[10-14] and the interactions of corneal and internal aberrations in the eye.[15]

During cataract surgery, the crystalline lens is replaced by an artificial IOL. The optical quality of the eye is determined by the combination of corneal and new internal aberrations. Several studies have reported that optical quality decreases with age.[10-14] Although a significant part of the degradation is caused by an increase in scattering,[16] some is caused by the shift of the spherical aberration of the crystalline lens towards less negative or even more positive values, which add to the positive corneal spherical aberration.[11]

Aberrometry has been recently applied to measure total and corneal aberrations in patients implanted with standard spherical IOLs.[3] Barbero et al[3] showed a slight increase of

From Instituto de Optica, Consejo Superior de Investigaciones Científicas (Marcos, Barbero); and Fundación Jiménez Díaz, (Jiménez-Alfaro), Madrid, Spain.

The authors acknowledge support from Comunidad Autónoma de Madrid, Grants # CAM08.7/004.1/2003 and GR/SAL/0387/2004; Ministerio de Ciencia y Tecnología Grant # BFM2002-02638; Ministerio de Educación y Cultura; Predoctoral Fellowship to S. Barbero; and Alcon Research Labs, Ft Worth, Tex.

The authors have no proprietary interest in the materials presented herein.

Correspondence: Susana Marcos, Instituto de Optica, CSIC, Serrano 121, 28006 Madrid, Spain. Tel: 34 915616800; Fax: 34 915645557; E-mail: susana@io.cfmac.csic.es

Received: March 29, 2004

Accepted: October 14, 2004

corneal aberrations with cataract surgery and higher amounts of aberrations (both spherical and other terms) in pseudophakic eyes compared with normal young eyes. The corneal findings expand previous reports that attributed the increased corneal astigmatism in pseudophakic eyes to the incision.[17,18] The increased total aberrations result in a degradation of the ocular modulation transfer function, although less than previously reported from double-pass measurements.[19,20] Although the increased positive spherical aberration of the IOL (measured both in vivo and in vitro, and simulated from lens designs) played a significant role in reducing optical quality, the presence of coma (attributed to tilt and decentration of the IOL) also was important.

New aspheric IOLs are nominally designed to produce negative spherical aberration,[21] attempting to reproduce the balance between corneal and internal aberrations found in young eyes.[11] The evaluation of these new lenses has been mostly done through theoretical and physical eye modeling and measurements of visual performance (visual acuity and contrast sensitivity). Kershner[22] found that uncorrected visual acuity 1 month after surgery was not significantly different between the aspheric group and the spherical-acrylic group. The most significant differences between aspheric and spherical lenses occurred at medium and high spatial frequencies (6-18 c/°) at mesopic levels. Retinal image contrast was measured indirectly from fundus images. These measurements describe the changes of visual performance and improvements of fundus visibility with cataract surgery, which are presumably associated with the presence or absence of intraocular scattering. However, they cannot directly correlate the differences across lenses with their individual aberration patterns.

Packer et al[23] also reported higher contrast sensitivity in patients with aspheric IOLs, except for low spatial frequencies (1.5-3 c/°) under mesopic conditions and high spatial frequencies (6-18 c/°) under photopic conditions. Mester et al[24] measured both visual performance and wave aberrations bilaterally in patients implanted with an aspheric IOL in one eye and a spherical IOL in the contralateral eye. Best corrected high-contrast visual acuity was not significantly different between the two groups, although low-contrast visual acuity was slightly and significantly better in the aspheric group, as was photopic and mesopic contrast sensitivity. Measurements of corneal aberrations did not show significant changes in mean corneal spherical aberration with surgery, except for two third-order corneal Zernike coefficients, which changed significantly. Mean corneal spherical aberration was significantly positive, as was total spherical aberration with spherical lenses (approximately 0.02 µm higher than the mean corneal aberration for 4-mm pupil diameter and 1 month postoperatively), whereas mean total spherical aberration with aspheric lenses was not significantly different from zero. The study also reported slight changes in the mean visual performance and aberration coefficients from 1 to 3 months postoperatively.

In the present study, total, corneal, and internal aberrations are compared in eyes implanted with aspheric IOLs with retrospective measurements in eyes implanted with spherical IOLs. In vivo measurement of internal aberrations allows assessment of the optical performance of the IOL within the patient's eye. The individual comparison of corneal and internal aberrations permits eye-to-eye assessment of the balance between the two components. The aspheric lens is designed to minimize the impact of spherical aberration in optical quality. However, several theoretical and computational studies predict that tilt and decentration are more deleterious in aspheric than spherical surfaces.[25] This study also compares third-order aberrations and investigates the sources of coma in pseudophakic eyes. In addition, corneal aberration changes for the two groups are discussed. Most studies in the literature report best spectacle-corrected visual performance in eyes with different types of IOLs, typically for far distance. However, out-of-focus performance in pseudophakic eyes[19] unable to accommodate is of interest. In fact, efforts are being made to design multifocal IOLs with enlarged depth-of-field but good in-focus optical quality, aiming at providing unaided patients with a range of near and far vision. In the present study, through-focus optical performance[26] is assessed with simulations of retinal image quality and modulation transfer functions are computed from the individual wave aberrations. Out-of-focus performance and optical depth-of-field of these two types of lenses are compared.

PATIENTS AND METHODS

Patients

Nine eyes of seven patients (mean age: 70.6±9 years, range: 51 to 81 years) implanted with spherical IOLs were reported in a previous study.[3] Ten eyes of five patients with bilateral cataracts (mean age: 65.6±17.3 years, range: 36 to 79 years) were randomly selected to participate in this study and implanted with aspheric IOLs. Patients were implanted bilaterally with the same type of lens. Selection criteria included good general health, no ocular pathology, and no complications

during surgery. All enrolled patients were informed on the nature of the study and provided informed consent that had been approved by the Institutional Review Board and the Declaration of Helsinki.

Pre- and Postoperative Evaluation

Patients received a comprehensive ophthalmic evaluation at the hospital (Fundación Jiménez Díaz) prior to enrollment to the study and surgery. The examination included uncorrected visual acuity (UCVA) and best spectacle-corrected visual acuity (BSCVA), biomicroscopy, keratometry, tonometry, and indirect ophthalmoscopy. Axial length and anterior chamber depth were determined with the Axis II ultrasonic biometer (Quantel Medical, Clermont-Ferrand, France), using a contact probe with fixation light. The IOL power was calculated with the SRK-T formula, always selecting the closer value to emmetropia.

Additional preoperative measurements were also conducted at the Instituto de Optica, CSIC, Madrid, Spain, which included corneal topography (Atlas Mastervue; Humphrey-Zeiss, San Leandro, Calif), corneal aberrations, optical biometry (IOLMaster, Humphrey-Zeiss), autorefractometry (Automatic Refractor Model 597, Humphrey-Zeiss), and when possible, total aberrations.

Postoperative evaluations at the hospital were conducted 1 day, 1 week, 1 month, and 3 months after surgery, and included UCVA and BSCVA, manifest refraction, biomicroscopy, keratometry, tonometry, and indirect ophthalmoscopy. Postoperative measurements at the Instituto de Optica were done 87±35 days after implantation of the spherical IOL and 125±25 days after implantation of the aspheric IOL. Although the aspheric group was measured on average 1 month later than the spherical group, results from our previous study[3] suggest that no change is expected over that time. These measurements included corneal topography, optical biometry, and autorefractometry with commercial instruments, and corneal and total aberrations using custom software and a prototype developed at the laboratory, respectively.

Surgical Technique

All procedures were performed by the same surgeon (I.J-A.) on an outpatient basis under topical anesthesia. The same procedure was used to implant the spherical and aspheric IOLs. A 3.2-mm clear corneal incision and a paracentesis were performed with a surgical knife. A 6-mm continuous curvilinear capsulorhexis was made under viscoelastic material. Phacoemulsification of the lens was performed with the Storz Premiere (Storz Instruments, St Louis, Mo) venturi system. After removing cortical material, the anterior and posterior capsules were cleaned with the automatic I-A straight tip. The incision was prolonged to 4.1 mm for the implantation of a foldable posterior chamber aspheric silicone lens Tecnis Z-9000 (Pfizer Ophthalmology, New York, NY) or the Acrysof spherical acrylic lens (Alcon, Ft Worth, Tex). Once the viscoelastic material was removed, the incision was closed by hydration, without sutures. Postoperatively, patients were treated with a combination of antibiotic and corticosteroid drops (dexametasone and tobramycin) for 4 weeks.

Corneal Aberrations

Corneal elevation maps were obtained using a videokeratographer (Atlas Mastervue). Wave aberrations of the anterior corneal surface were obtained by virtual ray tracing using an optical design program (ZEMAX; Focus Software, Tucson, Ariz) on corneal elevation data. Figure 1 shows a typical Placido ring image (A), the corresponding elevation map fit to a 7th order Zernike expansion (B), and the corresponding corneal wave aberration map (C) for eye 1, which was implanted with an aspheric IOL. A detailed description of the procedure, computations, and validation of the technique have been reported previously.[27-29]

Total Aberrations

Total wave aberrations were measured with a laser ray tracing technique. The principles and general implementation of the technique have been described in detail previously.[30-32] In this technique, a laser beam samples the pupil sequentially (Fig 1D), while the corresponding aerial images of light reflected off the retina are captured on a high resolution scientific-grade digital camera. The relative centroid coordinates of these aerial images are proportional to the partial derivatives of the wave aberration. Figure 1E represents the joint plot of centroids (spot diagram) for eye 1 (aspheric IOL). Measurements in eyes with spherical lenses were obtained using a first-generation of the instrument, whereas eyes with aspheric lenses were measured using a new prototype. Cross-calibrations of the instruments using trial lenses, phase-plates with known high order aberrations, and real eyes with various amounts of aberrations showed that both instruments provided similar data, within the measurement variability. The new instrument provides simultaneous capture of both retinal and pupil images, allowing to track the entrance beam locations at the pupil plane. Both front- and back-infrared illumination pupil images allow visualization of the pupil margins and, in most cases, the IOL edge.

Measurements were done on dilated pupils (typi-

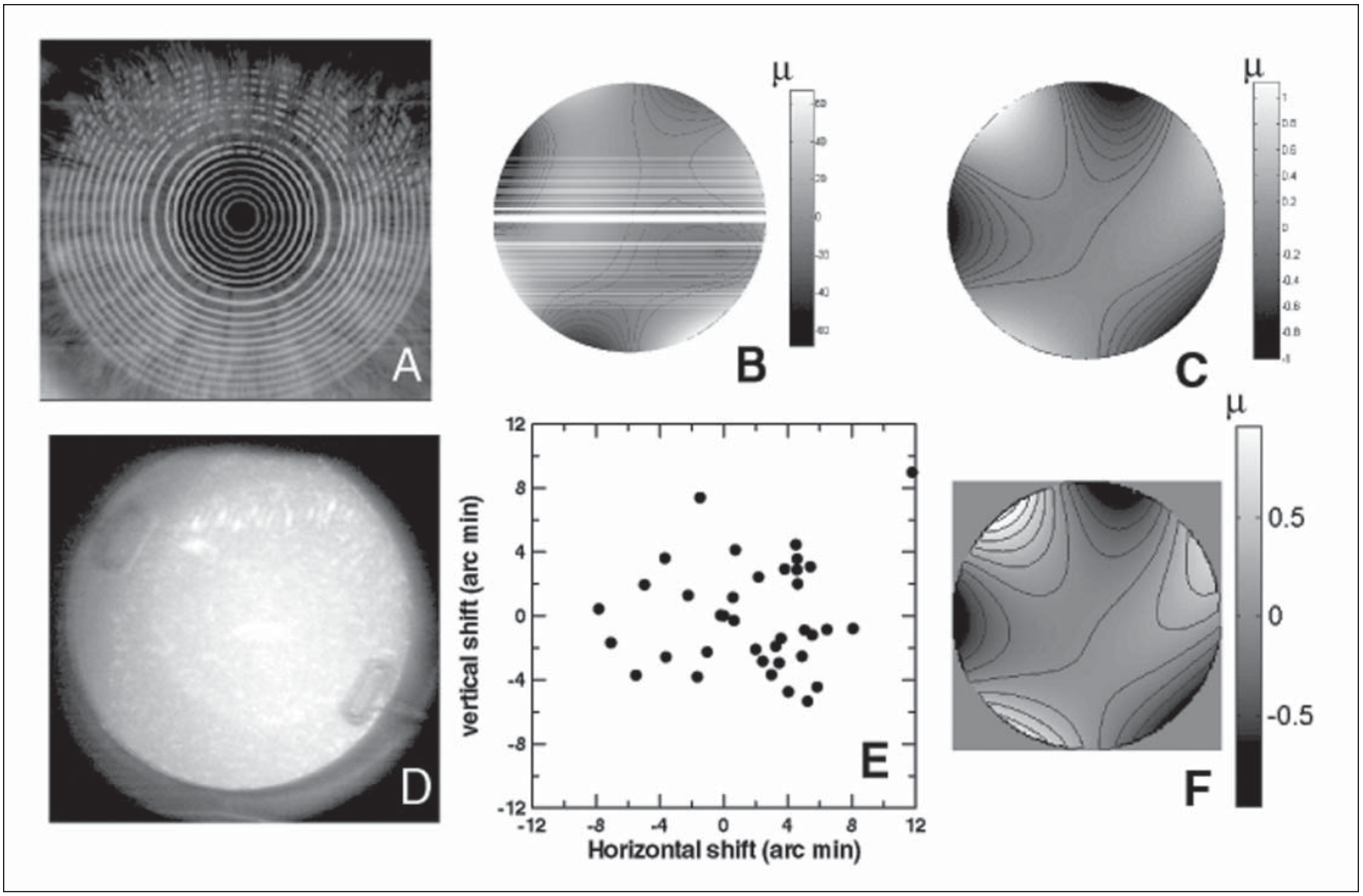

Figure 1. Corneal aberrations estimated from corneal topography of eye 1 implanted with an aspheric IOL. **A)** Placido Disk raw image. **B)** Corneal elevation map fit to a Zernike polynomial expansion. **C)** Corneal wave aberration pattern after virtual ray tracing and recentration. Total wave aberrations are measured using laser ray tracing. **D)** Back-illumination infrared pupil image showing the pupil and IOL edges and the entry location of the beam sampling the pupil. **E)** Spot diagram computed from the centroids of the retinal images corresponding to each entry pupil. **F)** Total wave aberration map estimated from the spot diagram.

cally ranging from 4.5 to 6 mm). Pupil dilation was achieved using one drop of tropicamide 1%. The number of sample points in the pupil was 37 in all cases, therefore the step size ranged from 0.75 to 1.00 mm. The illumination source was a fiber-coupled near infrared laser diode (786 nm).[33] Maximum energy exposure was 95 μW, at least one order of magnitude below safety levels of the American National Standard Institute for this wavelength.[34]

The wave aberration is reconstructed using a modal fitting to a Zernike polynomial expansion (6th order, ie, 28 terms for this study). The Zernike polynomial notation followed the recommendations of the Optical Society of America Standard Committee.[35]

Internal Aberrations

Internal aberrations were computed by subtracting corneal wave aberrations from total wave aberrations. Corneal elevation maps are typically referred to the first Purkinje image. For this reason, we used a realignment algorithm to ensure proper registration of the total aberration (which is measured with respect to the line of sight) and the corneal aberration map.[27-29,36] Internal aberrations stand for aberrations of the IOL (for a converging beam, as produced by the cornea) and posterior corneal surface aberrations. In normal and aphakic eyes, the latter have been shown to be negligible.[28]

Optical Quality Metrics

Wave aberrations were described in terms of individual Zernike coefficients or root-mean-square (RMS) wavefront error corresponding to single or several orders. Point-spread-function (PSF) and modulation transfer function (MTF) were computed using Fourier optics from wave aberrations, assuming homogenous pupil transmission. Through-focus MTF was computed shifting the defocus term in the Zernike polynomial expansion. The Strehl ratio, defined as the volume under the MTF normalized to the diffraction-limited MTF, excluding spatial frequencies beyond 45 c/°, was

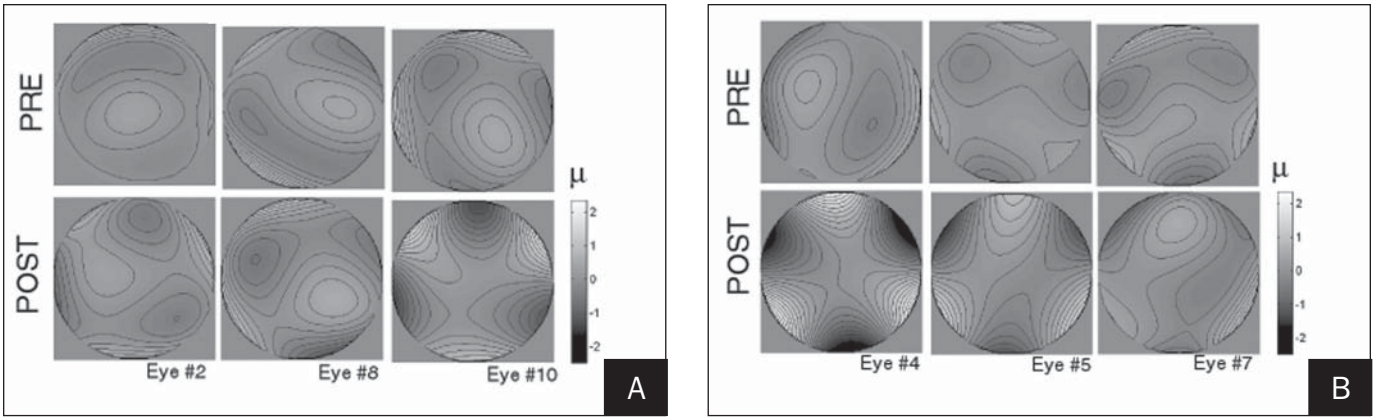

Figure 2. Examples of corneal wave aberration patterns (referred to the corneal reflex) in eyes before and after implantation of **A)** spherical and **B)** aspheric IOLs (pupil diameter: 4.5 mm). Postoperative corneal wave aberration maps show in general an increase in the amount of aberrations compared to the preoperative maps. Note the presence of trefoil in several postoperative corneal maps (both with aspheric and spherical IOLs), which was not seen preoperatively.

used as a retinal image quality metric. Simulations of ETDRS visual acuity charts were performed by convolution with the PSF, with appropriate scaling. All computations were performed for 4.5-mm pupil diameter, the smallest pupil for which data were available.

RESULTS

Change of Corneal Aberrations After IOL Implantation

Figure 2 shows typical examples of corneal wave aberrations before and after spherical and aspheric IOL implantation, referred to the first Purkinje image. Corneal changes were found in all eyes after implantation, with a more systematic tendency in eyes with aspheric IOLs with a 4.1-mm incision. All eyes except one changed from against-the-rule astigmatism (flatter vertical meridian, within $-10°$ to $+13°$) to astigmatism at 45°. Postoperative corneal astigmatism was in general symmetric across right and left eyes. Corneal third and higher order RMS increased by 0.11 ± 0.09 μm in eyes with spherical IOLs and 0.24 ± 0.21 μm in eyes with aspheric IOLs (the latter being statistically significant, $P=.007$). The largest increase occurs for trefoil terms (0.16 ± 0.13 μm and 0.27 ± 0.31 μm for spherical and aspheric IOLs, respectively, being statistically significant for the latter, $P=.01$). Figure 2 shows that postoperative higher order aberration patterns are dominated by trefoil terms. Corneal spherical aberration decreased slightly but significantly ($P<.05$) for spherical and aspheric IOLs (-0.04 ± 0.012 μm and -0.03 ± 0.012 μm, respectively).

Total, Corneal, and Internal Aberrations With Spherical and Aspheric IOLs

Figure 3 demonstrates corneal, total, and internal aberrations for a typical postoperative eye after spherical IOL implantation (eye 8) and aspheric IOL implantation (eye 1) for a 4.5-mm pupil diameter. Total aberration in the spherical IOL eye is dominated by positive spherical aberration (from the cornea and IOL) and coma (likely from tilt and decentration), and the total aberration in the aspheric IOL eye is dominated by trefoil (primarily of corneal origin). Figure 4 shows corneal, total, and internal mean RMS values for different orders, for aspheric (white) and spheric (gray) IOLs, for 4.5-mm pupils, all referred to the center of the pupil. When second order astigmatism terms are included (Fig 4A), optical quality with spherical IOLs significantly ($P=.02$) exceeds the optical quality with aspheric IOLs. Third and higher order RMS (Fig 4B) are significantly lower ($P=.03$) with aspheric IOLs compared with spherical IOLs. Third order RMS (Fig 4C) is not significantly different between the two groups. Fourth order RMS (Fig 4D) is significantly ($P=.002$) lower in aspheric than in spherical IOLs, due to significant differences in the spherical aberration.

Figure 5 shows the fourth order spherical aberration in all eyes with spherical and aspheric IOLs for 4.5-mm pupil diameters. All eyes except two with spherical IOLs show positive internal spherical aberration (average 0.14 ± 0.13 μm) and all show positive total spherical aberration (average 0.22 ± 0.07 μm). On the other hand, all eyes with aspheric IOLs show negative internal spherical aberration (-0.086 ± 0.057 μm) and total spherical aberration not significantly different from zero (-0.008 ± 0.049 μm). Differences in postoperative total and internal spherical aberrations between the two groups are statistically significant ($P<.001$). Differences between postoperative corneal spherical aberration between the two groups (0.089 ± 0.092 μm and 0.078 ± 0.078 μm for the spherical and aspheric IOL groups, respectively) are not statistically significant.

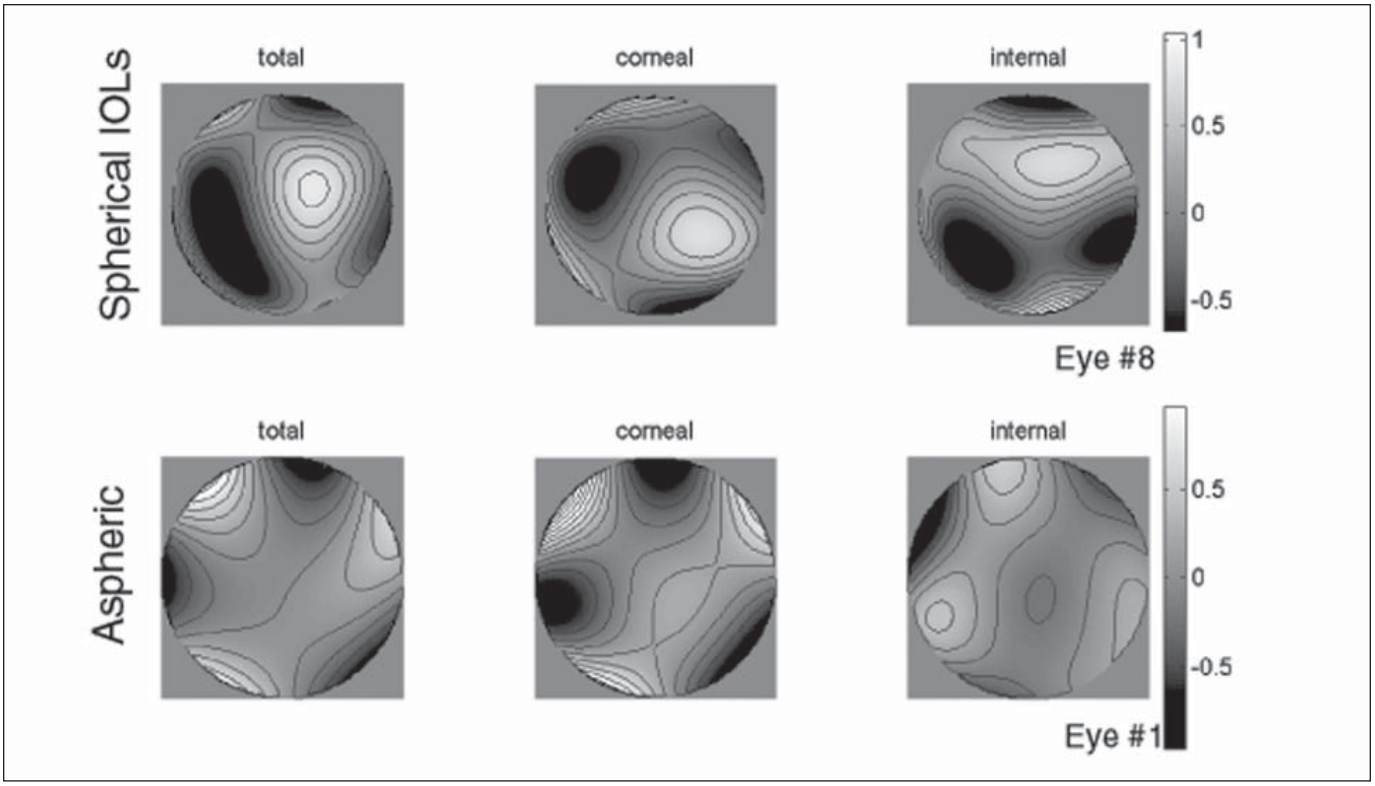

Figure 3. Examples of total, corneal, and internal wave aberration patterns (referred to the pupil center) in eyes after implantation of spherical and aspheric IOLs (pupil diameter: 4.5 mm). Note that the total wave aberration map in the eye with the spherical IOL shows additive features from the corneal and internal wave aberration maps, whereas the total wave aberration map in the eye with the aspheric IOL shows lower spherical aberration than corneal and internal aberrations individually.

Depth-of-field With Aspheric and Spherical IOLs

Root-mean-square wavefront error is useful to describe optical quality, but other metrics have been described to correlate better with visual performance.[37,38] When aberrations are not very high, Strehl ratio is useful to describe retinal image quality, as it takes into account both aberrations and diffraction, as well as complex interactions between aberrations. Figure 6 shows Strehl ratio versus RMS (both computed for third and higher order aberrations) for all postoperative eyes. Although the correlation between the two metrics is very high ($r=-0.90$, $P=.0002$ for spherical lenses; $r=-0.94$, $P<.0001$ for aspheric lenses), Strehl ratio appears to be more sensitive than RMS (showing differences between aspheric and spherical IOL performance with significant P values of 0.0018 and 0.03 for Strehl ratio and RMS, respectively).

Figure 7 shows Strehl ratio as a function of defocus for all study eyes. Gray lines indicate aspheric lenses and black lines indicate spherical lenses. Zero defocus stands for zero defocus term in the Zernike expansion, and the focus shift has been achieved by changing the defocus term (Z_2^0) by the corresponding amounts in microns. Negative defocus simulates placing negative lenses in front of the eye (or similarly placing the stimulus closer to the eye) and vice versa for positive defocus.

For illustration purposes and to compute the average through-focus curve, all curves were shifted laterally to overlap the maximum value. The maximum value of Strehl ratio is shifted by −0.05 diopters (D) (±0.39 D) for the aspheric lenses and −1.55 D (±0.30 D) for the spherical lenses. The larger shift for the spherical IOLs is due to spherical aberration and cross-quadratic terms in spherical aberration Zernike terms. The inset plot shows the average through-focus curves, with the maximum value shifted to zero defocus. This shift may be performed optically with the appropriate refractive correction, or by adjusting the IOL nomogram to obtain the optimal combination of spherical aberration and defocus. The average optical depth-of-field, computed as the focus range for which Strehl ratio does not fall below 80% of the maximum, is 1.26 D for the spherical lens and 0.88 D for the aspheric lens ($P=.0066$).

The optical definition of depth-of-field refers to relative quantities and this definition has also been traditionally adopted in the visual optics field.[26,39,40] However, referring to absolute quantities may be more

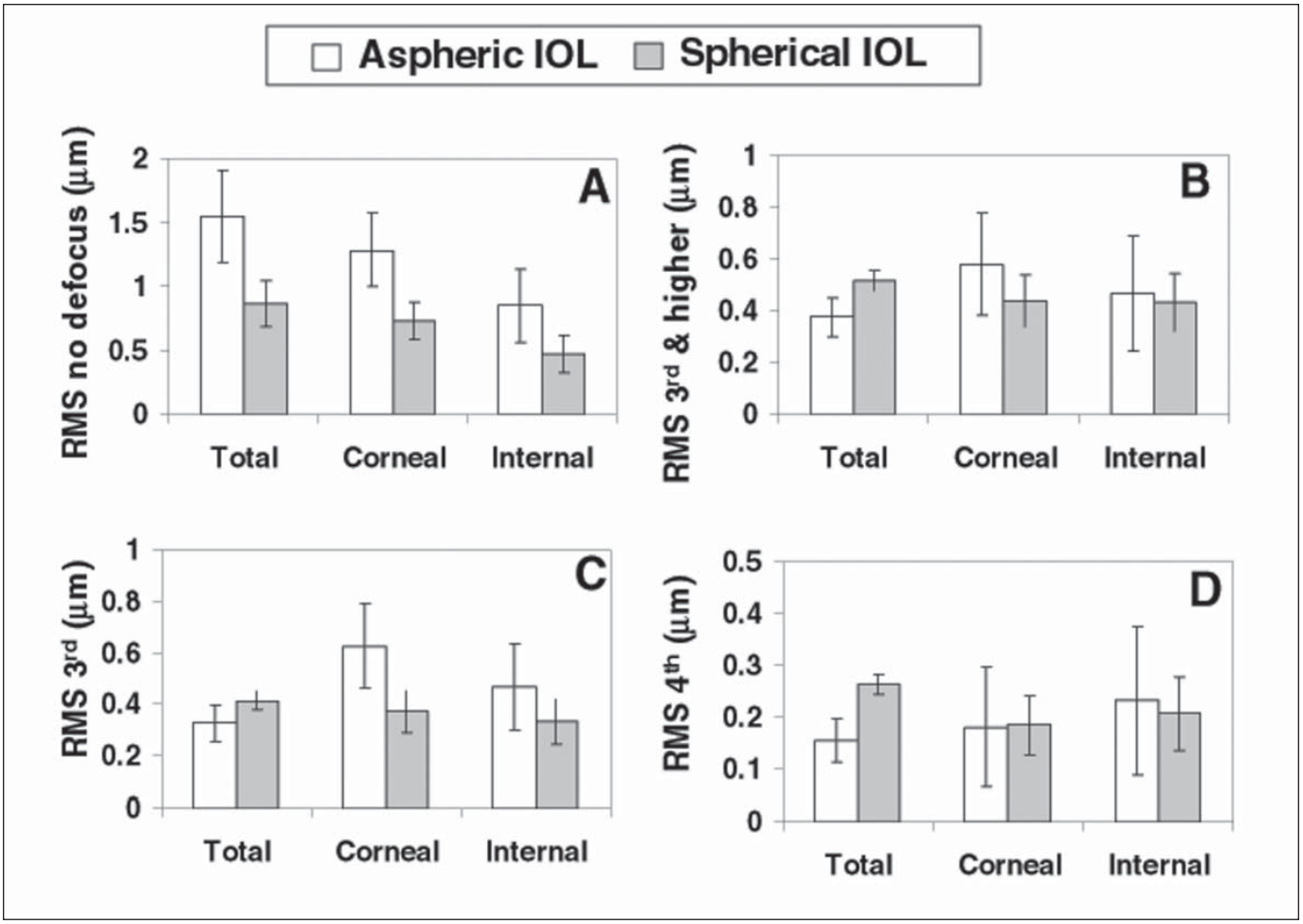

Figure 4. Comparison of optical performance, in terms of root-mean-square (RMS) wavefront error with aspheric (white bars) and spherical (gray bars) IOLs. Data are average of 10 eyes with aspheric IOLs and 9 eyes with spherical IOLs. Error bars represent standard deviations. **A)** RMS excluding tilt and defocus; **B)** RMS excluding tilt, defocus, and astigmatism; **C)** third order RMS; and **D)** fourth order RMS (pupil diameter: 4.5 mm).

informative when attempting to predict visual performance. The inset in Figure 7 shows that for a given optical correction that maximizes Strehl at 0.0 D and 4.5-mm pupil diameter, the absolute Strehl ratio is higher with spherical than with aspheric IOLs in a large negative focus range. Figure 8 shows that the average MTF at best focus is higher for aspheric (gray solid line) than for spherical IOLs at all spatial frequencies (black solid line). However, this situation is reversed for myopic defocus >1.0 D. (Figure 8 shows the MTF for −1.5 D, which is higher for the spherical IOL [gray dotted line] than for the aspheric IOL [black dotted line]).

Figure 9 shows the MTF ratios (spherical/aspheric). For best focus and a focus shift of −0.5 D, the ratio is <1.0, indicating better performance with the aspheric IOL. The shaded area indicates the range for which the average MTFs are within 80% of each other, indicating that these differences are optically (in the sense of the Raleigh criterion) significant beyond 5 c/° for best focus and 15 c/° for −0.5 D. For a defocus of −1.5 D (or similarly a stimulus at 66 cm), contrast modulation with spherical IOLs significantly exceeds that of the aspheric IOL. This difference increases for larger amounts of negative defocus (or similarly closer targets). The MTF and the definition of depth-of-field based on Strehl ratio refer to contrast difference, but do not take into account phase effects in the optical transfer function. Simulations of retinal images for two representative eyes (see Fig 9) show better optical quality at optimal focus for an aspheric lens than for a spherical lens. However, quality degrades more rapidly with defocus for aspheric than for spherical IOLs. On average, we found that the dioptric range for which the 20/20 line of the simulated retinal images of the ETDRS chart was legible was 1.5 D for the spherical IOL and 1.1 D for the aspheric IOL.

DISCUSSION

The sources of aberrations in patients implanted with spherical IOLs have been discussed previously.[3]

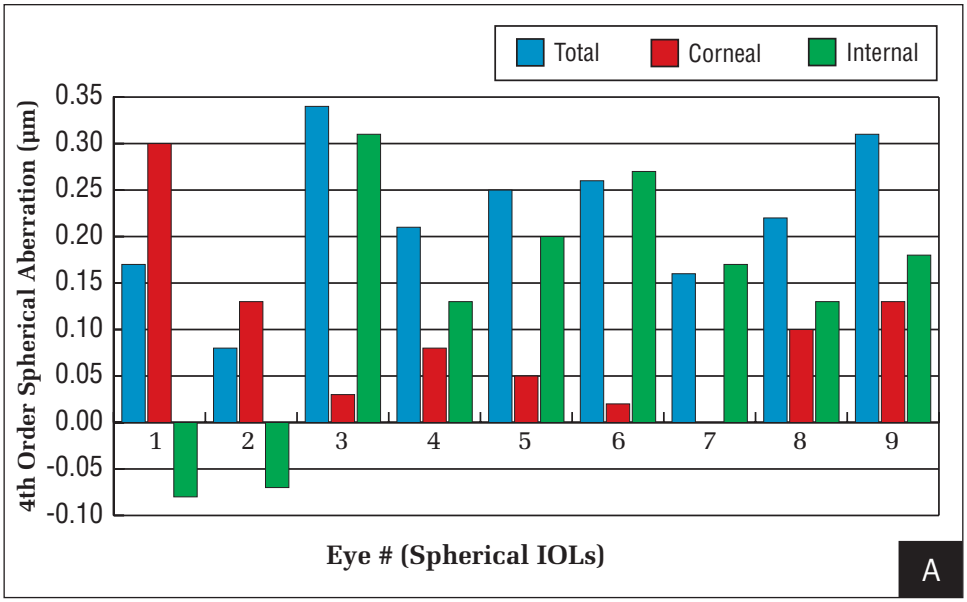

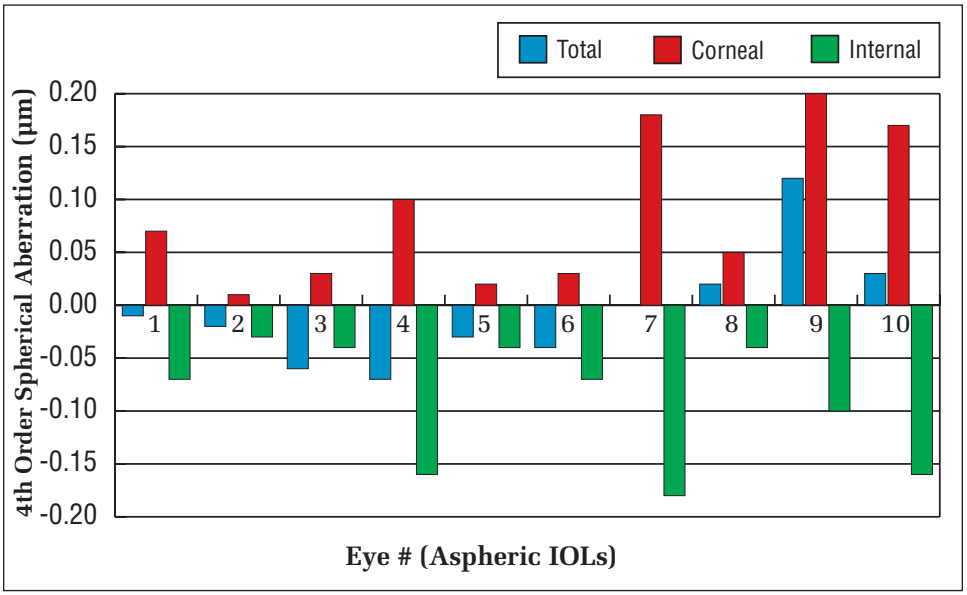

Figure 5. Total, corneal, and internal spherical aberration for eyes with **A)** spherical IOLS and **B)** aspheric IOLS (pupil diameter: 4.5 mm).

Spherical aberration is increased in patients implanted with spherical IOLs (0.20 µm more on average than in young eyes, and 0.23 µm more on average than in patients with aspheric IOLs). The spherical aberration is inherent to the design of the spherical IOL. In vivo and in vitro measurement as well as computer simulations showed that spherical aberration increased with IOL power.[3] The average spherical aberration in patients with aspheric IOLs is close to zero, satisfying the aim of the design of those lenses to cancel the corneal spherical aberration of the average patient. Nominally, these lenses are designed with a constant spherical aberration. The spherical aberration of the aspheric IOL was negative in all cases (−0.086 µm for a 4.5-mm pupil) but less negative than its nominal value (−0.27 µm for a 6-mm pupil). The difference is primarily due to pupil diameter.

For appropriate comparison across eyes, we performed all computations for a 4.5-mm pupil, which was the smallest dilated pupil in our group of eyes. Several patients achieved larger pupils, up to 6 mm. Average spherical aberration for eyes 3, 4, 8, and 10 (5-mm pupil) was −0.12 µm, for eyes 1, 2, and 9 (5.5-mm pupil) was −0.16 µm, and for eyes 5 and 6 (6-mm pupil) was −0.15 µm. We found some variability in the measured internal aberration (0.13 µm for spherical IOLs and 0.057 µm for aspheric IOLs). We did not find a correlation between internal spherical aberration and IOL power, as we found with spherical IOLs, although the power range (21 to 24 D) in the aspheric group is nar-

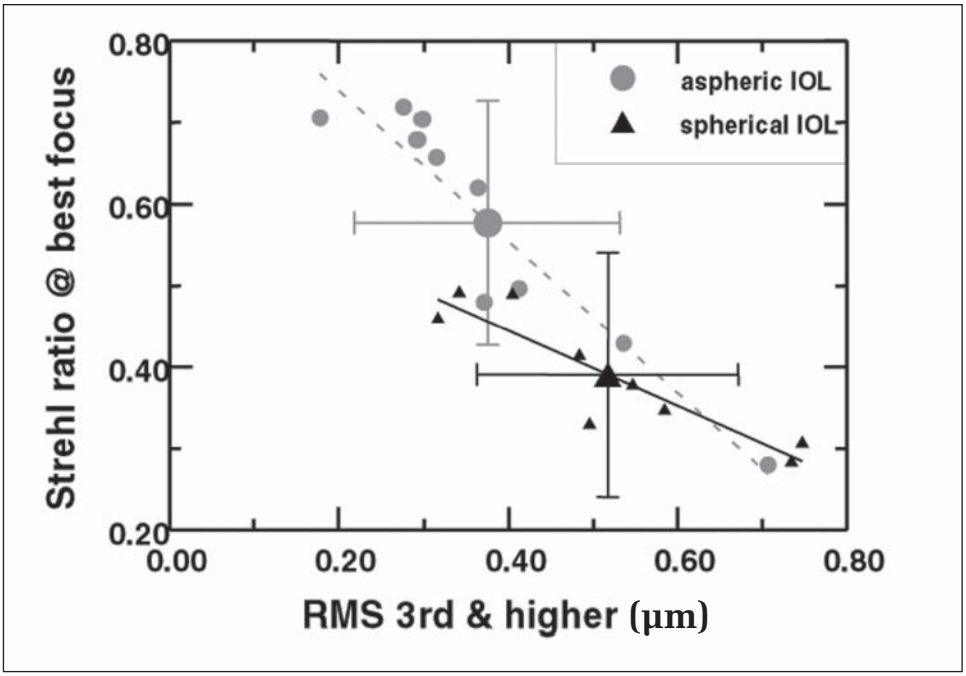

Figure 6. Root-mean-square (RMS) wavefront error vs Strehl ratio for third and higher order aberration in all eyes (n=9 spherical IOLs, n=10 aspheric IOLs) of the study (pupil diameter: 4.5 mm).

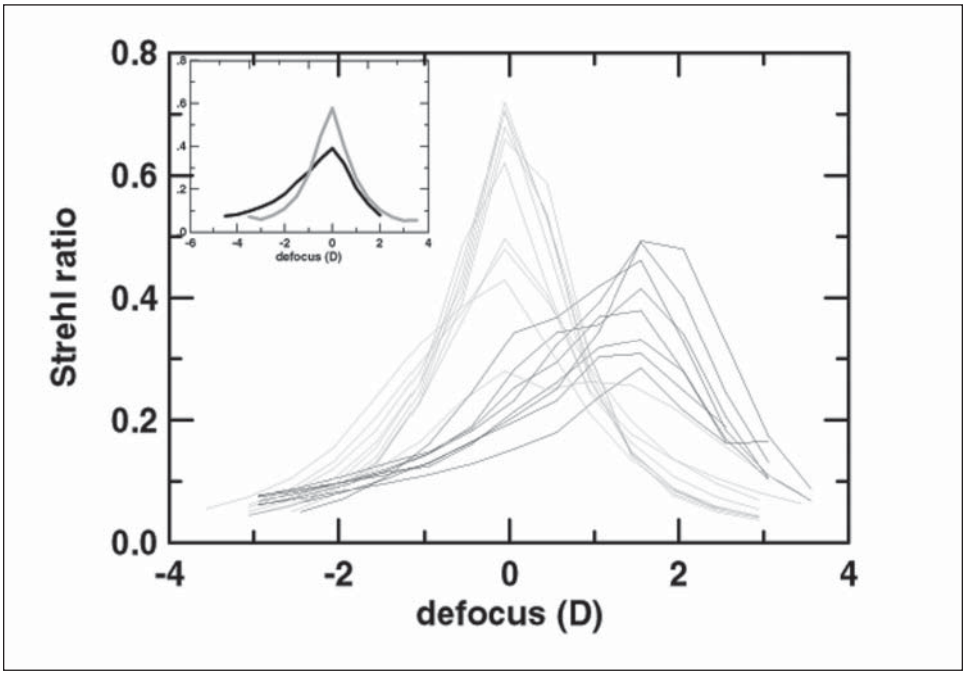

Figure 7. Strehl ratio as a function of defocus (shifted by changing the second order defocus term in the Zernike expansion) for all eyes of the study (spherical IOLs [n=9], black line; aspheric IOLs [n=10], gray line). Curves have been laterally shifted by −1.55 D and −0.05 D, respectively, which were average defocus shifts of spherical and aspheric IOLs, respectively. The inset plot represents average through focus Strehl ratio for spherical IOLs (thick black line) and aspheric IOL (thick gray line). The curves have been laterally shifted so that the maximum value corresponds to 0.0 D. Computations exclude astigmatism and are for 4.5-mm pupils. Negative values stand for negative defocus, ie, placing a negative correction in front of the eye.

rower than the spherical group (0 to 26 D). It should be noted that keeping the spherical aberration constant in a wide range of powers requires a careful control of the surface radii of curvature and, in particular, surface asphericity, which may impose a fabrication challenge. Also, because internal spherical aberration is estimated from the difference of total minus corneal aberration, it not only depends on the spherical aberration of the IOL, but on the actual position of the lens and the convergence of the rays refracted by the cornea.

We performed computer simulations using the actual corneal elevations in our group of eyes and axial lens position (from optical biometry measurements), which show that the effective internal aberration may vary by 10%. This effect is consistent with the variability of the effective IOL diameter viewed through the pupil. To our knowledge, only one other published study compares spherical aberration of spherical and aspheric IOLs for 4-mm pupils.[24] Although the trends are consistent with our data, the previous study found

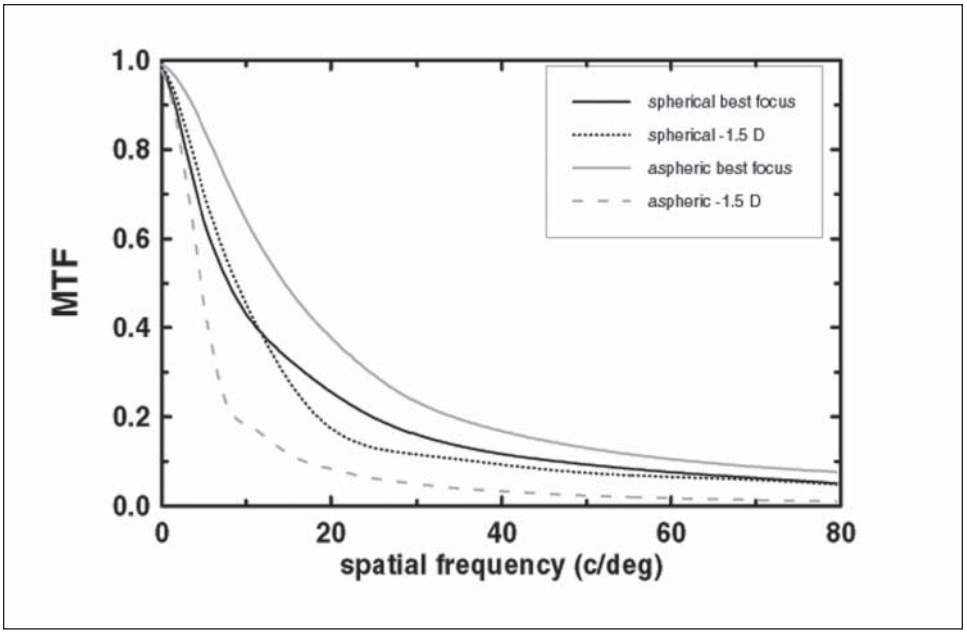

Figure 8. Modulation transfer function (MTF) in eyes implanted with spherical IOLs (average of 9 eyes) and aspheric IOLs (average of 10 eyes) for best focus and −1.5 D from best focus. Computations are based on individual experimental wave aberrations excluding astigmatism and are for 4.5-mm pupils.

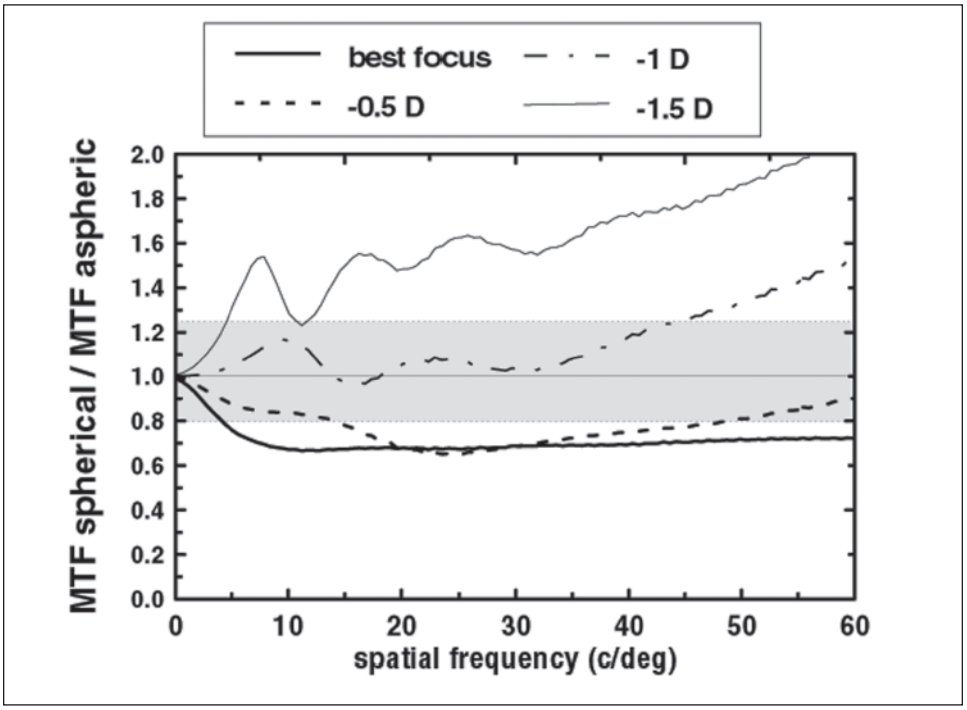

Figure 9. Ratio of spherical to aspheric MTF for best focus, and −0.5, −1.0, and −1.5 D from best focus, averaged across 9 eyes (spherical IOLs) and 10 eyes (aspheric IOLs). Values >1.0 are indicative of better performance by spherical IOLs and <1.0 are indicative of better performance by aspheric IOLs. The shaded area represents the range of spatial frequencies for which performance between the two types of lenses is within 80% of each other. Computations are based on individual experimental wave aberrations excluding astigmatism and are for 4.5-mm pupils.

lower absolute values for the internal spherical aberrations, both for the spherical IOL (~0.025 µm for 4-mm pupil vs 0.137 for 4.5-mm pupil in our study) and aspheric IOL (~0.047 µm for 4-mm pupil vs −0.086 µm for 4.5-mm pupil in our study).

Interestingly, we found that corneal spherical aberration decreased with the procedure, both after the spherical and aspheric IOL implantation. This difference was statistically significant, although probably of little optical and clinical significance. Mester et al[24] did not find a significant change of spherical aberration. In general, we found a significant corneal degradation with the procedure, particularly in the trefoil RMS. Mester et al[24] also found a significant increase in a trefoil term (C(3, −3)) after IOL implantation, as did Miller et al.[41] The causes for the increase in this term, possibly of corneal biomechanics origin, remain to be investigated, although it is likely that the amount of induced corneal aberration is correlated with the incision size.

Barbero et al[3] showed, using simulations and in vitro measurements on computer and physical eye models

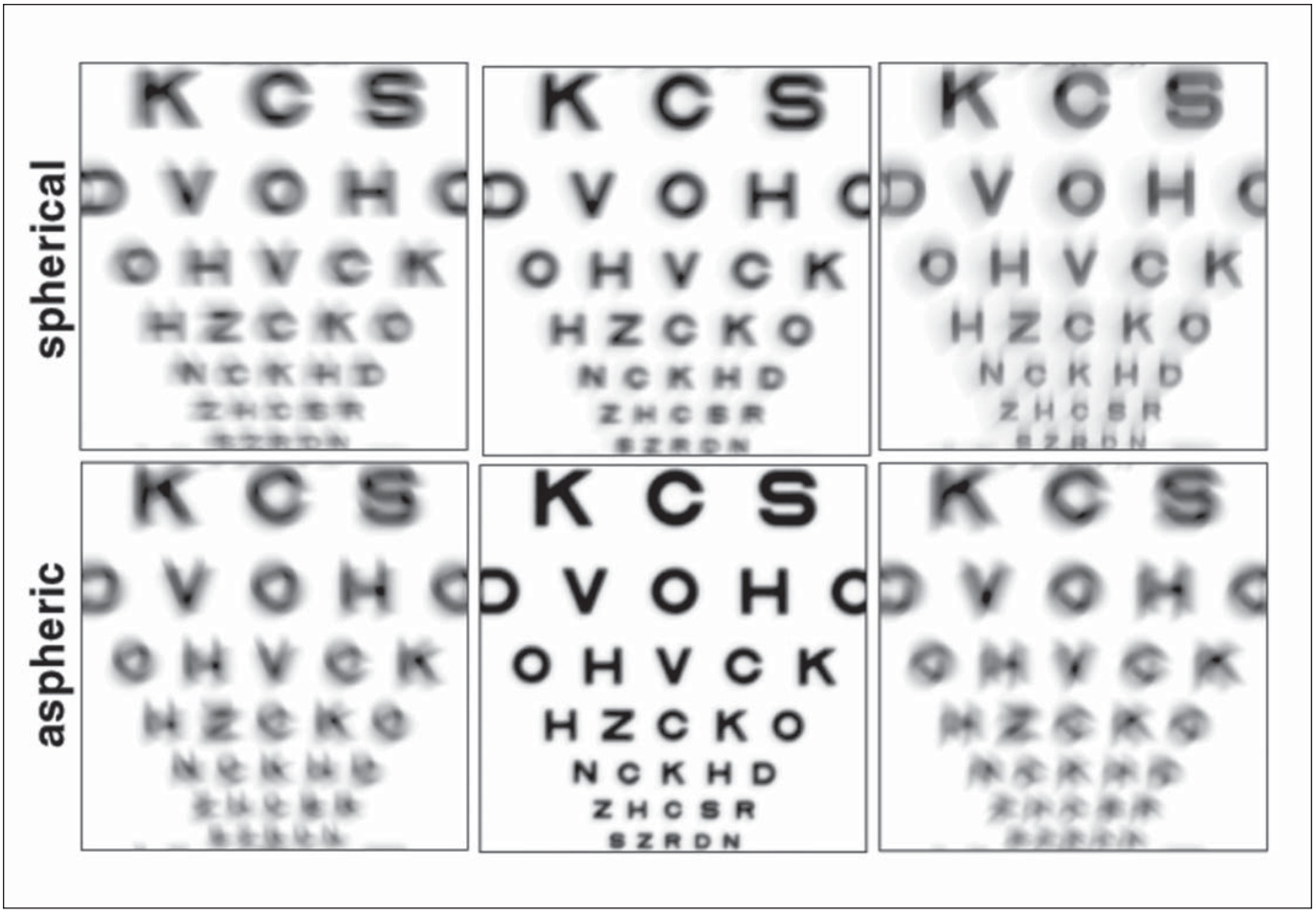

Figure 10. Simulation of retinal images of the ETDRS chart for two typical eyes (eye 8 with spherical IOL and eye 1 with aspheric IOL) for best focus and 1.0 D of positive and negative.

with spherical IOLs, that tilt and decentration induced third order coma, although the actual value depends on the specific combinations of tilt and decentration. It has been argued[25] that tilt and decentration would be more deleterious to optical quality with aspheric than spherical IOLs. In fact, a theoretical study by Holladay et al[21] showed that decentration >0.4 mm and tilt >7° would cancel the optical benefit of correcting spherical aberration. We did not find significant differences in third order aberrations between spherical and aspheric IOLs. Back-illumination pupil images were available in all patients with aspheric IOLs. In 7 of the 10 eyes, the edges of the IOL (see Fig 1) were clearly visible, at least partially, allowing estimation of the IOL center relative to the center of the pupil. The mean IOL decentration estimated from back-illumination images was 0.21±0.8 mm. We found that total vertical coma (Z_3^{-1}) was correlated (r=0.61) to a vertical decentration of the IOL (ranging from −0.18 to 0.17 mm). However, we did not find a correlation between horizontal coma and the horizontal coordinate, probably because tilt plays a major role in this orientation. A systematic measurement of tilt and decentration allows the individual impact on lens positioning on the actual wave aberration to be determined.

Our study shows a better in-focus performance of aspheric IOLs than spherical IOLs, confirming theoretical predictions of Holladay et al[3] and those of Mester et al.[24] In addition, our measurements show the effects of corneal incision and the actual lens position on optical performance. The improvement is only due to a reduction of spherical aberration. Third order aberrations are not significantly different across groups, and when astigmatism is included in the comparison, optical performance is similar across groups.

Eyes implanted with IOLs are unable to accommodate. The improvement of the cataract surgery procedure has run parallel to the efforts of providing the pseudophakic eye with multifocality and eliminating the dependence on optical correction for near tasks.

Multifocal IOLs aim at enlarging the depth-of-field, in most cases by reducing the optical quality at best focus, but providing the eye with acceptable optical quality in a wider focus range. The optical depth-of-field between spherical and aspheric IOLs has not been compared in vivo. Previous in vivo measurements of the optical depth-of-field in patients with IOLs (based on double-pass measurements of optical quality) were restricted to comparisons of multi- and monofocal IOLs.[19]

Our results can be compared to through-focus computations of optical quality using a physical eye model from the study by Holladay et al.[21] Our experimental measurements show similar average in-focus MTFs for the aspheric IOLs than the theoretical predictions of that study (0.59 for a 4.5-mm pupil and 0.62 for a 5-mm pupil, respectively, for 14 c/°, equivalent to 50 c/mm in the study by Holladay et al,[21] assuming a conversion factor of 280 µm/°[42]). However, our experimental in-focus MTFs for spherical IOLs are higher than Holladay's estimations (0.34 vs 0.24 for the same spatial frequency). The conclusion from Holladay et al[21] was that depth-of-field was not reduced with aspheric IOLs, although values were not reported. However, our estimations (using a global image quality metric rather than evaluating through-focus modulation at a single spatial frequency) show significantly lower optical depth-of-field with aspheric IOLs compared with spherical IOLs. Although for the focus range evaluated by Holladay et al[21] (±0.75 D) we also found that optical quality with aspheric IOLs is either better or not significantly lower than with spherical IOLs, our results suggest that tolerance to larger amounts of defocus is significantly higher for the spherical than the aspheric IOL. As a result, optical quality (both the MTF [see Figs 8 and 9] or simulated retinal images of acuity charts [Fig 10]) for defocus >1.00 D is significantly better with spherical IOLs. These differences increase with increasing spatial frequency and defocus (see Fig 9). The through-focus behavior with aspheric IOLs tends to be symmetric around the optimal focus. However, with spherical IOLs, optical quality for negative defocus tends to be better than for positive defocus (see Fig 7 inset). This asymmetry is also present in Holladay's through-focus estimations for a 3-mm pupil. Negative defocus is present when pseudophakic eyes corrected for infinity perform near tasks. From our optical measurements, best corrected eyes (for defocus and astigmatism) with spherical IOLs should perform better in near tasks than best corrected eyes with aspheric IOLs. Psychophysical measurements are needed to assess the visual importance of the measured differences in depth-of-field as well as the visual impact of correcting spherical aberration in residual defocus and astigmatism and surgery-induced high order aberrations.

REFERENCES

1. Mierdel P, Kaemmerer M, Krinke HE, Seiler T. Effects of photorefractive keratectomy and cataract surgery on ocular optical errors of higher order. *Graefes Arch Clin Exp Ophthalmol*. 1999;237:725-729.
2. Moreno-Barriuso M, Lloves JM, Marcos S, Navarro R, Llorente L, Barbero S. Ocular aberrations before and after myopic corneal refractive surgery: LASIK-induced changes measured with laser ray tracing. *Invest Ophthalmol Vis Sci*. 2001;42:1396-1403.
3. Barbero S, Marcos S, Jimenez-Alfaro I. Optical aberrations of intraocular lenses measured in vivo and in vitro. *J Opt Soc Am A Opt Image Vis Sci*. 2003;20:1841-1851.
4. Marcos S, Burns SA, Prieto PM, Navarro R, Baraibar B. Investigating sources of variability of monochromatic and transverse chromatic aberrations across eyes. *Vision Res*. 2001;41:3861-3871.
5. Marcos S. Aberrations and visual performance following standard laser vision correction. *J Refract Surg*. 2001;17:S596-S601.
6. He JC, Burns SA, Marcos S. Monochromatic aberrations in the accommodated human eye. *Vision Res*. 2000;40:41-48.
7. Cheng X, Bradley A, Hong X, Thibos LN. Relationship between refractive error and monochromatic aberrations of the eye. *Optom Vis Sci*. 2003;80:43-49.
8. Carkeet A, Luo HD, Tong L, Saw SM, Tan DT. Refractive error and monochromatic aberrations in Singaporean children. *Vision Res*. 2002;42:1809-1824.
9. Marcos S, Moreno-Barriuso E, Llorente L, Navarro R, Barbero S. Do myopic eyes suffer from larger amount of aberrations? Proceedings of the 8th International Conference on Myopia; July 7-9, 2000; Boston, Mass.
10. Guirao A, Gonzalez C, Redondo M, Geraghty E, Norrby S, Artal P. Average optical performance of the human eye as a function of age in a normal population. *Invest Ophthalmol Vis Sci*. 1999;40:203-213.
11. Artal P, Berrio E, Guirao A, Piers P. Contribution of the cornea and internal surfaces to the change of ocular aberrations with age. *J Opt Soc Am A*. 2002;19:137-143.
12. McLellan JS, Marcos S, Burns SA. Age-related changes in monochromatic wave aberrations in the human eye. *Invest Ophthalmol Vis Sci*. 2001;42:1390-1395.
13. Smith G, Cox M, Calver R, Garner LF. The spherical aberration of the crystalline lens of the human eye. *Vision Res*. 2001;15:235-243.
14. Calver RI, Cox MJ, Elliott DB. Effect of aging on the monochromatic aberrations of the human eye. *J Opt Soc Am A Opt Image Sci Vis*. 1999;16:2069-2078.
15. Artal P, Guirao A. Contributions of the cornea and the lens to the aberrations of the human eye. *Optics Letters*. 1998;23:1713-1715.
16. van den Berg TJ. Analysis of intraocular straylight, especially in relation to age. *Optom Vis Sci*. 1995;72:52-59.
17. Jacobs BJ, Gaynes BI, Deutsch TA. Refractive astigmatism after oblique clear corneal phacoemulsification cataract incision. *J Cataract Refract Surg*. 1999;25:949-952.
18. Rainer G, Menapace R, Vass C, Annen D, Findl O, Schmetterer K. Corneal shape changes after temporal and superolateral 3.0 mm clear corneal incisions. *J Cataract Refract Surg*. 1999;25:1121-1126.

19. Artal P, Marcos S, Navarro R, Miranda I, Ferro M. Through-focus image quality of eyes implanted with monofocal and multifocal intraocular lenses. *Optical Engineering*. 1995;34:772-779.
20. Guirao A, Redondo M, Geraghty E, Piers P, Norrby S, Artal P. Corneal optical aberrations and retinal image quality in patients in whom monofocal intraocular lenses were implanted. *Arch Ophthalmol*. 2002;120:1143-1151.
21. Holladay J, Piers P, Koranyi G, van der Mooren M, Norrby NE. A new intraocular lens design to reduce spherical aberration of pseudophakic eyes. *J Refract Surg*. 2002;18:683-691.
22. Kershner R. Retinal image contrast and functional visual performance with aspheric, silicone, and acrylic intraocular lenses: prospective evaluation. *J Cataract Refract Surg*. 2003;29:1684-1694.
23. Packer M, Fine IH, Hoffman RS, Piers P. Prospective randomized trial of an anterior surface modified prolate intraocular lens. *J Refract Surg*. 2002;18:692-696.
24. Mester U, Dillinger P, Anterist N. Impact of a modified optic design on visual function: clinical comparative study. *J Cataract Refract Surg*. 2003;29:652-660.
25. Atchison DA. Design of aspheric intraocular lenses. *Ophthalmic Physiol Opt*. 1991;11:137-146.
26. Marcos S, Moreno E, Navarro R. The depth-of-field of the human eye from objective and subjective measurements. *Vision Res*. 1999;39:2039-2049.
27. Barbero S, Marcos S, Merayo-Lloves J, Moreno-Barriuso E. Validation of the estimation of corneal aberrations from videokeratography in keratoconus. *J Refract Surg*. 2002;18:263-270.
28. Barbero S, Marcos S, Merayo-Lloves J. Corneal and total optical aberrations in a unilateral aphakic patient. *J Cataract Refract Surg*. 2002;28:1594-1600.
29. Marcos S, Barbero B, Llorente L, Merayo-Lloves J. Optical response to LASIK surgery for myopia from total and corneal aberrations. *Invest Ophthalmol Vis Sci*. 2001;42:3349-3356.
30. Navarro R, Losada MA. Aberrations and relative efficiency of light pencils in the living human eye. *Optom Vis Sci*. 1997;74:540-547.
31. Moreno-Barriuso E, Marcos S, Navarro R, Burns SA. Comparing laser ray tracing, the spatially resolved refractometer, and the Hartmann-Shack sensor to measure the ocular wave aberration. *Optom Vis Sci*. 2001;78:152-156.
32. Marcos S, Diaz-Santana L, Llorente L, Dainty C. Ocular aberrations with ray tracing and Shack-Hartmann wavefront sensors: does polarization play a role? *J Opt Soc Am A Opt Image Sci Vis*. 2002;19:1063-1072.
33. Llorente L, Diaz-Santana L, Lara-Saucedo D, Marcos S. Aberrations of the human eye in visible and near infrared illumination. *Optom Vis Sci*. 2003;80:26-35.
34. American National Standard Institute. American National Standard for the safe use of lasers, Standard Z-136.1-1993. Orlando, Fla: The Laser Institute of America; 1993.
35. Thibos LN, Applegate RA, Schwiegerling JT, Webb RH, VST Members. Standards for reporting the optical aberrations of eyes. In: *Trends in Optics & Photonics*. Vol 35. 2000:110-130.
36. Dorronsoro C, Barbero S, Llorente L, Marcos S. On-eye measurement of optical performance of rigid gas permeable contact lenses based on ocular and corneal aberrometry. *Optom Vis Sci*. 2003;80:115-125.
37. Guirao A, Williams DR. A method to predict refractive errors from wave aberration data. *Optom Vis Sci*. 2003;80:36-42.
38. Cheng X, Thibos L, Bradley A. Estimating visual quality from wavefront aberration measurements. *J Refract Surg*. 2003;19: S579-S584.
39. Legge GE, Mullen KT, Woo GC, Campbell FW. Tolerance to visual defocus. *J Opt Soc Am A*. 1987;4:851-863.
40. Charman W, Whitefoot H. Pupil diameter and the depth-of-field of the human eye as measured by laser speckle. *Optica Acta*. 1977;24:1211-1216.
41. Miller J, Anwaruddin R, Straub J, Schwiegerling J. Higher order aberrations in normal, dilated, intraocular lens, and laser in situ keratomileusis corneas. *J Refract Surg*. 2002;18:S579-S583.
42. Drasdo ND, Fowler CW. Non-linear projection of a retinal image in a wide-angle schematic eye. *Br J Ophthalmol*. 1974;58:709-714.